Available online at www.sciencedirect.com

SciVerse ScienceDirect

Ceramics International 38 (2012) 2253–2259

CERAMICS INTERNATIONAL

www.elsevier.com/locate/ceramint

Synthesis, characterization and evaluation of titanium carbonitride surface layers with varying concentrations of carbon and nitrogen

P.K. Ajikumar [a,*], M. Kamruddin [a], S. Kalavathi [a], A.K. Balamurugan [a], S. Kataria [a], P. Shankar [b], A.K. Tyagi [a]

[a] *Materials Science Group, Indira Gandhi Centre for Atomic Research, Kalpakkam, India*
[b] *Saveetha School of Engineering, Chennai, India*

Received 2 May 2011; received in revised form 18 October 2011; accepted 27 October 2011
Available online 4 November 2011

Abstract

Titanium carbonitride (TiCN) surface layers were grown by direct exposure of Ti to a gas mixture of ammonia and methane at 1050 °C. TiC_xN_{1-x} coatings with varying C/N ratio were synthesized by appropriately changing the content of methane and ammonia in the reactive gas mixture. The resultant layers were subjected to various characterization and evaluation techniques to study the variation of properties with respect to change in C/N ratio. A systematic change in lattice parameter and microstructure was observed as a function of the composition of active gas mixture. Friction coefficient of TiC was found to be extremely low (0.078). Reaction mechanisms for the growth of TiN and TiC were found to be entirely different. The effect of composition of the gas mixture on growth kinetics of TiCN is elucidated.

Keywords: Titanium carbonitride; Microhardness; Friction coefficient; XRD; SEM

1. Introduction

Transition metal carbides and nitrides, particularly of titanium, have attracted much attention due to their extraordinary mechanical and physical properties like high hardness, high melting point, and wear and corrosion resistance [1–3]. For tribological applications, the properties of interest are hardness, wear resistance, low coefficient of friction and chemical inertness. TiN and TiC, being isostructural (fcc) and totally miscible, the combination of the two in appropriate ratios could result in TiC_xN_{1-x} with properties incorporating the advantages of both TiC and TiN [4–6]. It has been shown that TiCN films have a lower wear rate (3–4 times) and lower coefficient of friction (5–7 times) than TiN films [5]. Better wear properties of TiCN compared to TiN is attributed to its higher hardness and the presence of carbon, which acts as a lubricant, resulting in reduced friction and wear [7,8]. Pure TiC coating suffers from spallation due to high internal compressive stress, whereas TiCN films offer good adhesion with the substrate as the internal stress in them is negligible [7]. Transition metal carbonitrides can be thought as an alloy of carbide and nitride. Thus, TiC_xN_{1-x} exists over a broad composition range, where "x" varies from 0 to 1 with a high fraction of vacancies occurring at non-metal atom sites. This compositional variation and vacancy concentration affect its thermodynamic, mechanical, electrical, magnetic and superconducting properties [1,9]. Though pure TiC is harder than pure TiN, it is reported that the maximum hardness is achieved at an optimum C/N ratio in the carbonitride phase [10,11]. However, a study by Veprek et al. [12] showed an approximately linear increase in the hardness of TiC_xN_{1-x} with increasing "x" value. The experimental and modeling studies of Bull et al. [13] could not unambiguously establish any linear or parabolic relationship between hardness and carbon content in TiC_xN_{1-x}. A theoretical study conducted by Jhi et al. [10] suggests that the hardness depends fundamentally on the electronic properties of nitrogen and carbon and the valence electron concentration of their combination.

Different methods like physical vapour deposition, chemical vapour deposition, diffusional carbonitriding, organo-metalic

* Corresponding author. Tel.: +91 4427480081; fax: +91 4427480081.
E-mail addresses: pkajikumar@gmail.com, aji@igcar.gov.in (P.K. Ajikumar).

0272-8842/$36.00
doi:10.1016/j.ceramint.2011.10.075

plasma immersion ion processing, arc evaporation, combustion synthesis etc. are being used for the synthesis of titanium carbonitride [14–19]. In this study, we investigate the gas phase synthesis of titanium carbonitride with varying concentrations of carbon and nitrogen on pure titanium surface using NH_3 and CH_4 as reactive gases. Several advantages of this method includes, feasibility to grow thicker layers (several microns), absence of a sharp interface between the modified layer and the substrate and the chemical purity of the transformed layer compared to other methods. TiCN layers can be grown on pure Ti by exposing the Ti substrate held at high temperature to a reactive gaseous atmosphere containing NH_3 and CH_4. The stoichiometry of the product layer can be varied by altering the ratio of NH_3 and CH_4.

2. Experimental details

The experimental facility and synthesis procedure employed in the study have already been reported in our earlier publications [20–22]. However, for completeness a brief description is given here. Pure Ti specimens (~12 mm × 12 mm × 1.6 mm) were metallographically polished and ultrasonically cleaned in acetone prior to carbo-nitridation. The experiments were carried out in a thermogravimetric analyzer–mass spectrometry (TGA–MS) system provided with mass flow controller based gas delivery to facilitate specimen exposure to a desired gas mixture. Prior to sample heating, the system was evacuated and purged with high pure Ar gas several times to minimize oxygen partial pressure. This was done to reduce surface oxidation. Other experimental conditions like gas flow and heating rates were optimized by previous experiments [20,21]. In addition to NH_3, CH_4 mixture, high pure Ar flow (flow rate = 45 standard cubic cm per minute, sccm) was also maintained through the TGA system to protect the microbalance. The in situ weight gain of the Ti specimen and change in concentrations of NH_3, CH_4 and other product gases were monitored by TGA and dynamic mass spectrometry, respectively as a function of exposure time and temperature. Temperature for carbo-nitridation of Ti was optimized by previous experiments at 1050 °C. Subsequently, a number of identically prepared specimens were exposed isothermally to $NH_3 + CH_4$ gas mixtures for 4 h each. The NH_3, CH_4 gas mixtures used were of composition 100:0, 80:20, 75:25, 65:35, 50:50, 35:65, 25:75, 20:80 and 0:100. The samples processed in these atmospheres are identified as C-0, C-20, C-25, C-35, C-50, C-65, C-75, C-80 and C-100, respectively, where C represent CH_4 and the number gives its percentage. The total flow of the two reactive gases was maintained at 4 sccm. The phase identification of the carbonitrided layers was carried out by X-ray diffraction (XRD, STOE X-ray Powder Diffractometer). The surface and cross sectional microstructures of the specimens were investigated using Scanning Electron Microscopy (SEM, Philips GX 30 ESEM). Elemental analysis of the surface layer was carried out by Secondary Ion Mass Spectrometry (SIMS, Cameca, France) in the depth profile mode. Evaluation of these layers for microhardness and friction coefficient was carried out by vickers hardness indenter (Leitz Wetzler, Germany) and tribometer (CSM Instruments, Switzerland), respectively.

3. Results and discussion

A typical TGA–MS spectra depicting the variations in specimen weight and the concentration of the reactive gas mixture as a function of time and sample temperature is shown in Fig. 1. The figure shows the reduction of partial pressure of NH_3 and CH_4 and the corresponding increase in partial pressures of product gases nitrogen and hydrogen with increase in temperature. Dissociation temperature of ammonia is less than that of methane and hence the release of hydrogen initiates from ammonia. The resultant weight gain due to the formation of titanium carbonitride is also seen from the graph. Fig. 2 presents the comparison of trends in weight gain during the formation of titanium nitride and titanium carbide upon treatment in pure ammonia and pure methane, respectively. The weight gain is normalized for better distinguishing the trends. The square of the normalized weight gains is also plotted in the same graph to comprehend the nature of the process. The difference in the weight gain trend on exposure to NH_3 and CH_4 can be clearly inferred from this figure. In the case of nitride, the rise in weight gain proceeds parabolically. This parabolic nature is also clear from the near linear relationship between the square of the weight gain and time. The isothermal region of the square of the weight gain profile is fitted to a straight line and is shown in Fig. 2. The parabolic nature was observed for all the specimens except the one which was treated in methane alone (sample C-100). The parabolic weight gain, which indicates the diffusion controlled nature of titanium nitride growth has already been reported by many researchers [23–25]. In the case of carbide, the weight gain follows a sigmoidal profile. Fig. 3 indicates the percentage weight gain per unit surface area of the nine specimens treated at 1050 °C for 4 h each to varying gas compositions. A systematic decrease in weight gain upon

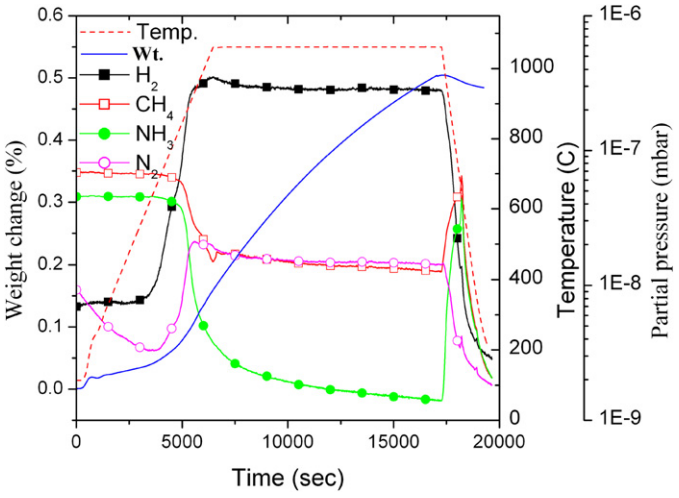

Fig. 1. Typical TGA–MS spectra showing dissociation of NH_3 and CH_4 with the release of hydrogen and nitrogen gases and the resultant weight gain due to formation of titanium carbonitride.

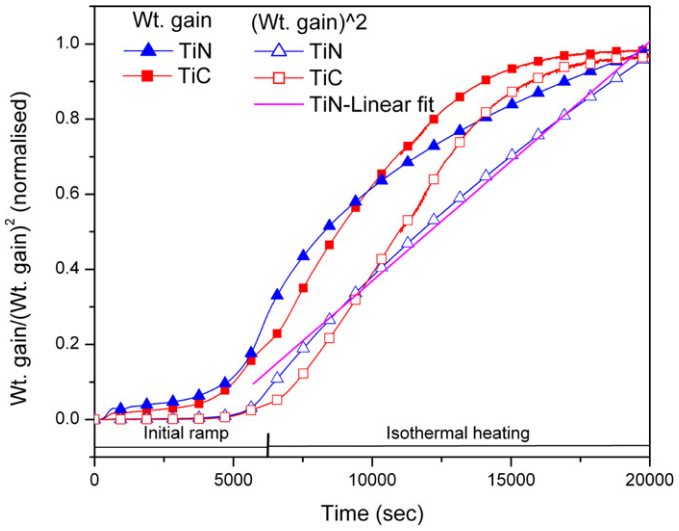

Fig. 2. The weight gain (normalized) trend upon nitridation and carburization of Ti at 1050 °C for 4 h. The square of the weight gain is also plotted.

exposure from 100% NH_3 to 20% NH_3 gas mixture (C-0 to C-80) and a sharp increase in the case of 100% CH_4 (C-100) can be observed.

The XRD spectra of the exposed specimens with an expanded theta range at the inset are presented in Fig. 4a. It clearly shows the formation of TiN, TiC and TiC_xN_{1-x} with varying gas mixtures (JCPDS Nos. 38-1420, 32-1383). Both TiN and TiC being iso-structural, only shift in peak positions is expected from XRD among TiC_xN_{1-x} compounds. The lattice parameters are also calculated from XRD peaks using the software supplied along with the STOE system and are plotted in Fig. 4b. Using Vegard's law [26], the carbon/nitrogen content was also estimated and plotted in Fig. 4b.

Fig. 5a–c shows the surface SEM micrographs of three specimens treated in pure NH_3, NH_3:CH_4 (50:50) and pure CH_4 atmospheres (samples C-0, C-50 and C-100). Fig. 5d–f shows the corresponding cross sectional SEM images of these specimens, respectively. The surface SEM shows a clear

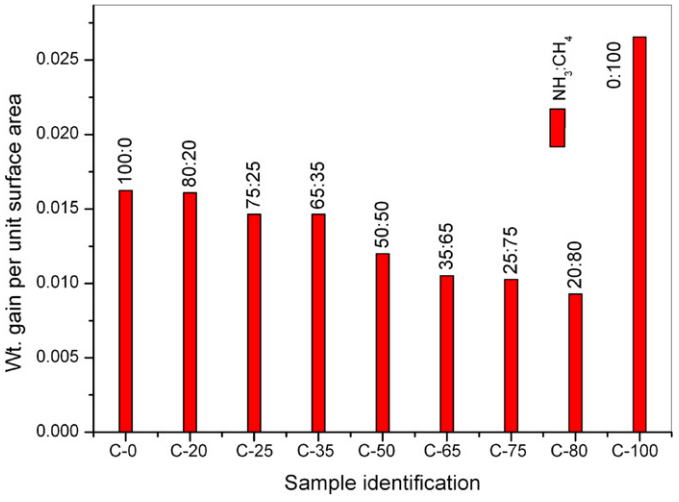

Fig. 3. Weight gain per unit area of specimens treated for 4 h at 1050 °C in different NH_3/CH_4 gas mixtures.

difference in morphology and reduction in grain size as a function of increase in carbon content. It can be observed that the grain size of pure TiN is about 5–10 μm and that of TiC is approximately 0.5 μm. The specimen exposed to 50:50 gas mixture (Fig. 5b) showed smaller grains compared to that of TiN. Surface cracks are visible on this sample. The corresponding cross sectional SEM of these specimens show that the thickness of the layer formed is about 15–25 μm. The cross section of sample C-0 is smooth while that of sample C-100 is highly porous. However, porosity of the sample C-50 (Fig. 5e) is confined to less than 5 μm thick outer layer.

The qualitative SIMS depth profiles of constituent elements carbon, nitrogen and oxygen of samples exposed to different gas mixtures are shown in Fig. 6. 20 keV cesium ions were used as the primary beam for the measurements. Elemental ions as well as cesium–metal ion clusters were detected in the mass spectrometer. It clearly indicates a systematic change in the concentration of carbon in accordance with the change in the CH_4 content in the exposure gas mixtures, but the changes are not that pronounced in the case of nitrogen. Oxygen profile was taken to estimate the level of oxygen impurities in the carbonitride layer.

Mechanical evaluation of the carbonitride layer was carried out by measuring the microhardness and friction coefficient of the samples. A vickers microindentor was used for the measurement of hardness with an applied load of 50 g. In order to overcome the hindrance of surface roughness in making accurate hardness measurements, all the specimens were subjected to mild surface polishing prior to hardness measurement. So the measured values would be lower than the actual values because of the graded nature of the surface layers. Starting from TiN, almost a linear increase in hardness was observed in samples with increasing carbon content (Table 1). All the measured values are less than the reported data and are attributed to the removal of the hardest outermost layer during polishing. Hardness values were also measured along the cross section using the same indentor with an applied load of 15 g. Measurements were made from a distance of 10–100 μm from the surface. Some of the hardness profiles along the cross section are shown in Fig. 7. Tribological behaviour of coatings was investigated using a tribometer in linear reciprocating mode. Si_3N_4 ball of 6 mm diameter was used as static counter body. A normal load of 5 N and a constant sliding velocity of 3 cm/s were maintained for all the measurements. The experiments were conducted without lubrication and the humidity was controlled within 60 ± 5%. The average friction coefficient is tabulated in Table 1 and the variation of friction as a function of number of laps is shown in Fig. 8.

Since the onset temperature of ammonia dissociation is lower compared to that of methane, there is a possibility for the formation of a thin layer of nitride prior to carbide formation. Such a layer could limit further growth diffusion controlled. Comparing the weight gain per unit surface area of the specimens treated in different atmospheres (Fig. 3), it is observed that a reduction in weight gain from pure NH_3 (sample C-0) to 20% NH_3 (sample C-80) and a sharp increase in case of pure CH_4 (sample C-100). The intake of the active species

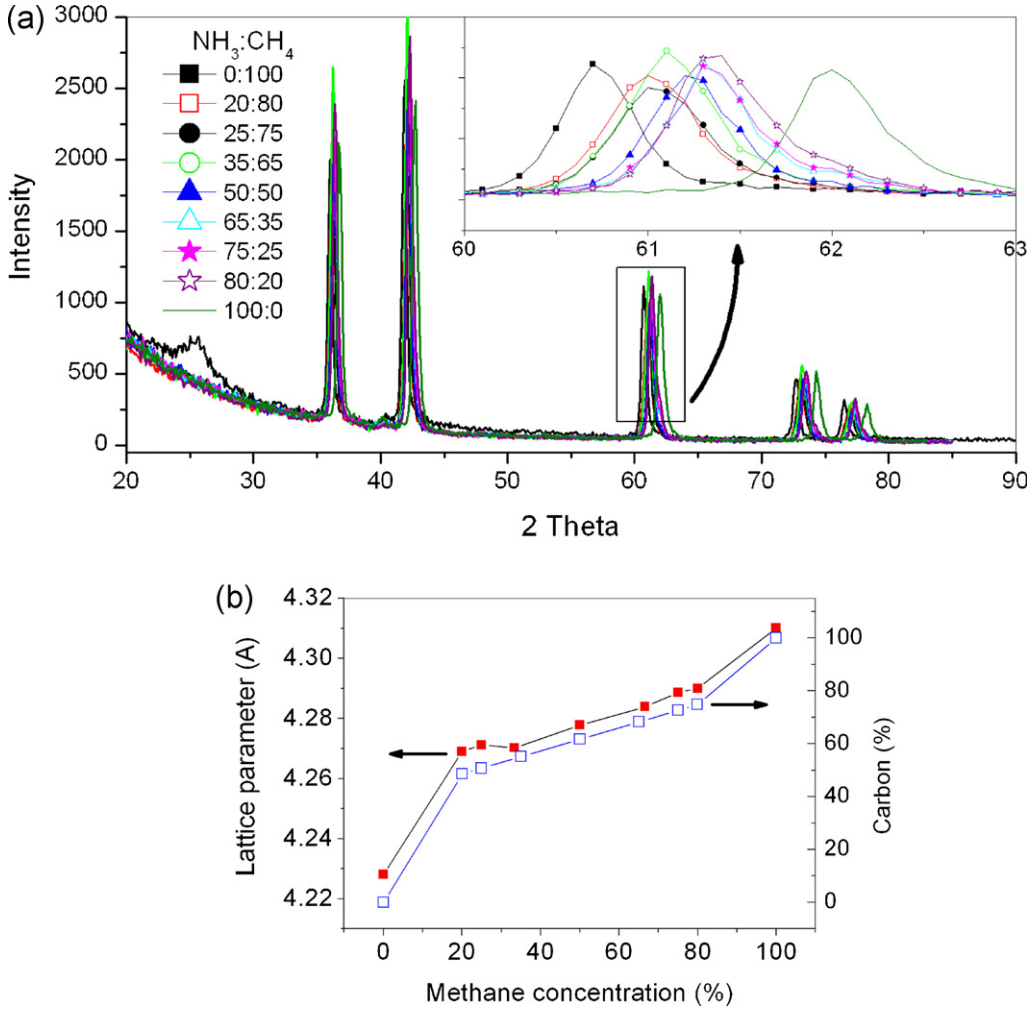

Fig. 4. (a) XRD patterns of carbonitrided Ti specimens showing peak shift due to lattice expansion with an expanded pattern at the inset. (b) Calculated lattice parameters and concentration of carbon estimated using Vegard's law as a function of NH_3/CH_4 ratio.

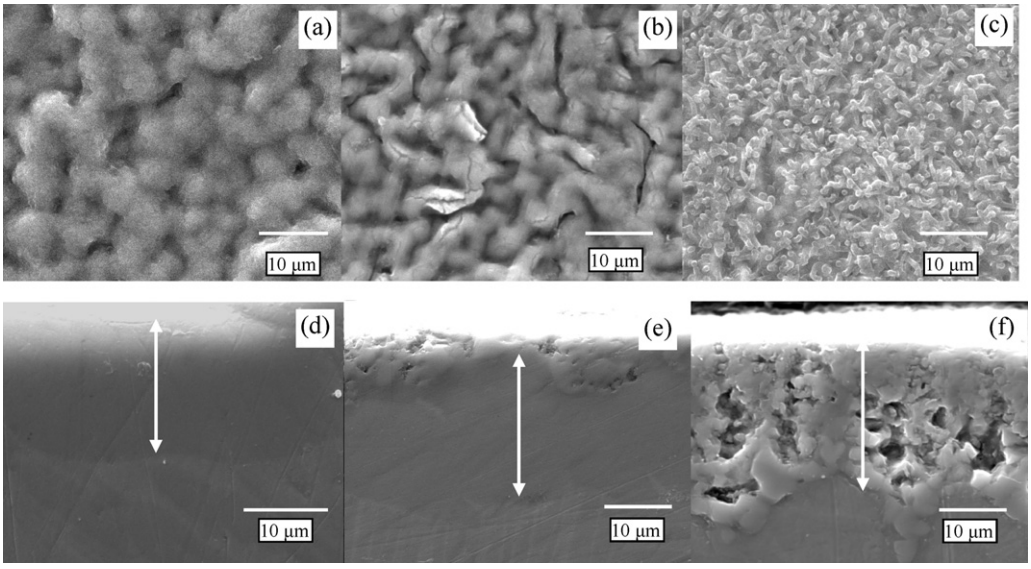

Fig. 5. Surface morphology (a–c) and cross sectional microstructure (d–f) of samples C-0, C-50 and C-100, respectively by SEM.

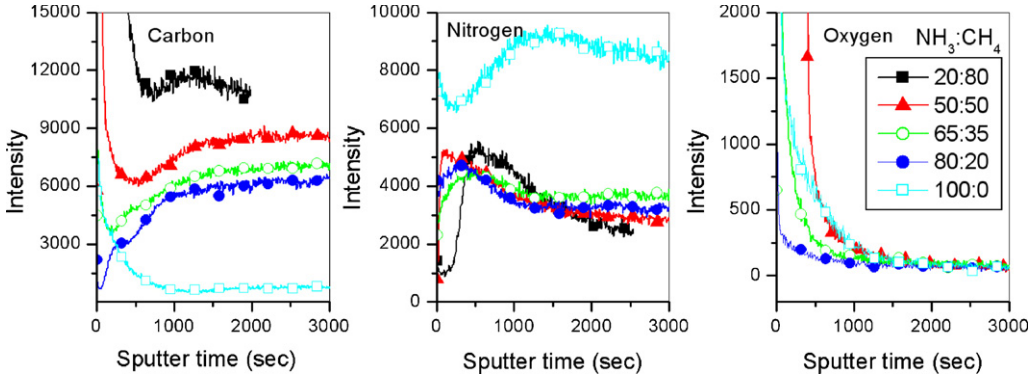

Fig. 6. SIMS elemental profile for carbon, nitrogen and oxygen as a function of sputter time for Ti samples treated in different gas mixtures.

Table 1
Variation of hardness and average value of friction coefficient (μ) with gas mixture.

	Sample id								
	C-0	C-20	C-25	C-35	C-50	C-65	C-75	C-80	C-100
Hardness (VHN)	1303	1427	1439	1443	1563	1607	1613	1726	1889
μ (mean)	0.377	0.403	0.434	0.403	0.42	0.38	0.32	0.363	0.078

reduces with the ammonia content in the gas mixture. This exceptional behaviour could be attributed to the initial nitride layer formation as mentioned earlier. Generally TiN is an excellent diffusion barrier compared to TiC [27]. It is an established fact that TiN act as a diffusion barrier for carbon and this property of TiN had been used by Weiser et al. [28] for chemical vapour deposition of diamond. TiN is also used extensively as a diffusion barrier coating in semiconductor industry [27]. Hence the initial nitride layer restricts the carbon diffusion into the sample and the growth process is mainly controlled by the availability of nitrogen at the reaction interface. The availability of nitrogen reduces with the reduction in ammonia content in the gas mixture. When the active gas is only CH_4 (sample C-100), carbide formed is very porous in nature (Fig. 5f) and the growth process no longer depend only on diffusion as the porosity provides a lot of short cuts for the transport of carbon and hence resulted in higher rate of growth. In addition to this, the grain size is also too small for TiC (Fig. 5c) compared to that of TiN (Fig. 5a) which would result in higher mobility for carbon atoms through grain boundaries since the grain boundary diffusion is much faster compared to bulk diffusion [29].

XRD investigations (Fig. 4a) confirm the formation of TiCN with varying concentration of carbon and nitrogen. Absence of peaks other than that corresponds to fcc TiC_xN_{1-x} in the observed XRD patterns (except corresponds to C-100) confirms the purity of the phase formed. The pattern corresponds to TiC showed an additional broad peak around 25°, which indicates the presence of graphitic carbon at the surface. Formation of titanium oxide, which is observed in many other synthesis processes, is below the X-ray detection limit in our case due to the presence of reducing atmosphere of hydrogen, a decomposition product of both NH_3 and CH_4. Also, the ratio of intensities of all the five peaks in the observed range is almost matching with JCPDS data which indicates that there is no texturing in the formed carbonitride layers. When the composition changes from pure nitride to carbonitride, the lattice expands due to bigger size of carbon atoms and it results in the shifting of peaks towards lower angles. The lattice expansion is almost linear for all the specimens excluding TiN and TiC, when plotted against percentage methane gas, as seen from the graph (Fig. 4b). Since lattice parameters of TiN and TiC differ only by about 2%, we can apply Vegard's law [26] for estimation of the concentration of nitrogen and carbon in the surface layer of TiC_xN_{1-x}. This was done after fitting the lattice parameters of samples C-20 to C-80 linearly, leaving the two extreme points. For TiN and TiC, carbon content is assumed to

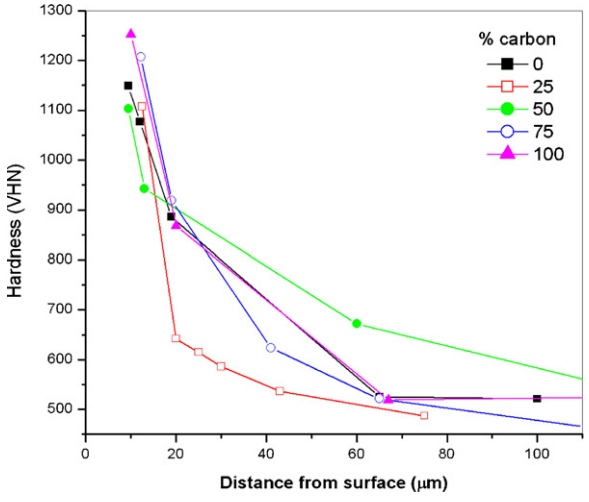

Fig. 7. Variation of hardness along the cross section of the Ti samples treated in different gas mixtures.

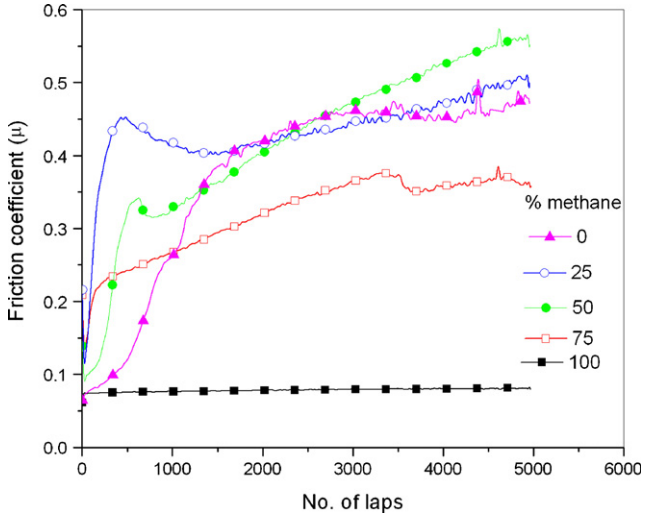

Fig. 8. The variation of friction coefficient against number of laps for some of the Ti specimens treated in different NH_3/CH_4 mixtures.

be 0% and 100%, respectively. The calculated values of x are plotted against methane gas composition in Fig. 4b. The minimum value of x is found to be 0.48 and maximum 0.75 corresponding to methane gas ratios 20% and 80%, respectively. X-ray scattering intensity exponentially reduces as a function of depth [30] and the major contribution to intensity would be from the top surface of the sample. Hence, the above result shows that the outermost region of the formed layer is carbon rich carbo-nitride. This is also evident from the cross sectional microstructure (Fig. 5e), where the outer region of the formed layer is porous with similar microstructure as that of TiC (Fig. 5f). Also, diffusion and solubility of nitrogen is higher compared to that of carbon in titanium [31,32]. Thus nitrogen may diffuse deep into the sample and form a carbon deficient carbonitride, leaving a carbon rich layer at the outermost surface. Hence, the C/N ratio changes with respect to depth too. This could be the reason for the higher values of carbon concentration calculated using Vegard's law. The morphology and grain size of TiC (sample C-100) is markedly different from that of other samples with a grain size of about 0.5 μm. This is due to the higher nucleation density of carbide compared to nitride, which result in smaller grain size. The surface of sample C-0 (TiN) is free from any cracks due to slow and stress free growth of nitride, but for other carbonitrided samples (samples C-20 to C-80), cracks are visible and this could be due to concomitant growth of TiC and TiN which results in the development of stress on the layer. This is evident from cross section SEM images also. For pure TiN (Fig. 5d), the interface is pore free and smooth, but for TiC (Fig. 5f), the cross section is porous. Also, for TiC the thickness of the converted layer is more compared to other samples in agreement with the weight gain results (Fig. 3). The cross section SEM of the sample carbonitrided at NH_3:CH_4 of 50:50 ratio shows the microstructure close to that of the carburized sample (sample C-100) at the topmost layer, whereas the microstructure below is close to that of the nitrided sample (sample C-0) indicating a carbon rich surface and nitrogen rich inner regions.

The qualitative SIMS analysis of the specimens revealed a systematic change in concentration profiles of carbon as a function methane concentration. In the case of nitrogen, this systematic is not very evident. The maximum depth probed was measured to be about 1 μm using a surface profilometer. From the estimation of carbon content (Fig. 4b), and from the cross sectional microstructure (Fig. 5d–f) it is clear that the outermost surface is carbon rich carbonitride. This could be the reason for the pronounced changes in carbon profile of SIMS (Fig. 6) with respect to change in reactive gas mixture. Since the outer surface is nitrogen deficient, the changes in nitrogen profile are not very apparent with the corresponding change in ammonia concentration in the active gas mixture. Combining the XRD, SEM and SIMS observations, one can unambiguously conclude that the carbon to nitrogen ratio in the carbonitrided layer change with the active gas mixture ratio. Over and above this, from the Cross section SEM microstrucures and XRD investigations, it is clear that a variation of C/N ratio exist as a function of depth in each specimens leaving a carbon rich layer at the outermost surface and nitrogen dominant layer beneath. The oxygen concentration (Fig. 6) was found to be dropping drastically beyond near surface indicates the superior quality of the layers formed. The initial high oxygen signal near the specimen surface could be from absorbed oxygen or moisture.

The measured microhardness values (Table 1) show a systematic increase in hardness with methane concentration. These values are less than the reported data [2] due to the removal of the outermost layer by surface polishing. Contrary to the reported observations by Jhi et al. [10] and Karlsson et al. [11], we did not find a maximum hardness for any intermediate composition between 100% nitrogen and 100% carbon. This can be attributed to the graded nature of the surface layers in which composition of carbon and nitrogen changes as a function of depth. It was attempted to measure the variation of hardness along the cross section of the specimens also (Fig. 7). The thickness of the carbo-nitrided layer is in the range of 20–25 μm. Microhardness measurements are not practical closer than 10 μm from the surface. Hence only the values measured within 10–25 μm from the surface are the valid data points. Hence a strong dependency on C/N ratio could not be ascertained from this measurement. The evaluation of frictional properties shows a distinct behaviour for TiC sample compared to other specimens (Table 1). While all other specimens showed average coefficient of friction (μ) around 0.4, TiC (C-100) showed an extremely low value of 0.078. This value is comparable to that of graphite ($\sim$0.05) and we assume that graphitic carbon is present on the surface of TiC. The XRD spectrum corresponds to TiC (Fig. 4a) show a broad peak around 25°, which corresponds to nanocrystalline graphite. The lamellar structure of graphite like carbon shears easily due to weak van der Walls forces existing between the basal planes and give a lubricating effect which in turn results in reduced friction and wear [7,8]. The variation of friction coefficient as a function of no. of cycles for some of the specimens is shown in Fig. 8. The friction coefficient of TiC remains constant through out the experiment indicating its lower wear rate. For other specimens, friction coefficient is higher and

also it increases with number of laps. The increase in friction coefficient with respect to number of cycles should be due to the removal of the formed layers due to wear and exposure of Ti metal to the tribo-contact.

4. Conclusions

Titanium carbonitride surface layers with varying concentration of carbon and nitrogen were synthesized by gas phase thermochemical process with ammonia and methane as active gases. The online measurement of weight change revealed the difference in growth mechanisms of nitride and carbide. The converted layer thickness was found to be 15–25 μm. XRD investigations revealed the formation of phase pure TiN, TiC and TiC_xN_{1-x} surface layers. There was systematic shift in XRD peak positions as a function of the ratio of the reactive gas mixture indicating corresponding change in C/N ratio. Variation in lattice parameter due to the change in C/N ratio was estimated from XRD data. Change in microstructure and grain size was revealed by surface and cross section SEM. Grain size of the layers varied from ∼10 μm to ∼0.5 μm for TiC_xN_{1-x} (x = 0–1). Over and above the decreases in non-metal atom content as a function of depth, variation of carbon to nitrogen ratio exists in each carbonitrided specimens as a function of depth. The outer surface is carbon rich leaving a nitrogen rich layer beneath. TiC was found to be the hardest and having lowest friction coefficient. Hardness increase was almost linear with increase in carbon content in the specimens. Average friction coefficient was found to be drastically reduced for pure TiC (0.078), which is comparable to that of graphite.

Acknowledgements

The authors acknowledge Mr. Thomas Paul, Dr. Tom Mathews, Dr. Rajagopalan, Dr. Sitaram Dash and Dr. Ramaseshan for very useful suggestions and help during the present work. The authors also acknowledge the support of Dr. C.S. Sundar, Director, MSG.

References

[1] L.E. Toth, Transition Metal Carbides and Nitrides, Academic, New York, 1971.
[2] J.E. Sundgren, H.T.G. Hentzell, A review of the present state of the art in hard coatings grown from the vapor, J. Vac. Sci. Technol. A 4 (1986) 2259–2279.
[3] H. Holleck, Material selection for hard coatings, J. Vac. Sci. Technol. A 4 (1986) 2661–2669.
[4] E. Erturk, O. Knotek, W. Burgmer, H.G. Prengel, H.J. Heuvel, H.G. Dederichs, C. Stossel, Ti(C,N) coatings using the arc process, Surf. Coat. Technol. 46 (1991) 39–46.
[5] E. Vancoille, J.P. Celis, J.R. Roos, Tribological and structural characterization of a physical vapour deposited TiC/Ti(C,N)/TiN multilayer, Tribol. Int. 26 (1993) 115–119.
[6] R. Bertoncello, A. Casagrande, M. Casarin, A. Glisenti, E. Lanzoni, L. Mirenghi, E. Tondello, TiN, TiC and Ti(C, N) film characterization and its relationship to tribological behaviour, Surf Interface Anal. 18 (1992) 525–531.
[7] O. Knotek, F. Loffler, G. Kramer, Arc deposition of Ti–C and Ti–C–N using acetylene as a reactive gas, Vacuum 43 (1992) 645–648.
[8] Yeong Yan Guu, Jen Fin Lin, Chi-Fong Ai, The tribological characteristics of titanium nitride, titanium carbonitride and titanium carbide coatings, Thin Solid Films 302 (1997) 193–200.
[9] J.E. Sundgren, Structure and properties of TiN coatings, Thin Solid Films 128 (1985) 21–44.
[10] S.-H. Jhi, J. Ihm, S.G. Louie, M.L. Cohen, Electronic mechanism of hardness enhancement in transition-metal carbonitrides, Nature 399 (1999) 132–134.
[11] L. Karlsson, L. Hultman, M.P. Johansson, J.-E. Sundgren, H. Ljungcrantz, Growth, microstructure, and mechanical properties of arc evaporated TiC_xN_{1-x} ($0 \leq x \leq 1$) films, Surf. Coat. Technol. 126 (2000) 1–14.
[12] S. Veprek, M. Haussmann, S. Reiprich, Li. Shizhil, J. Dian, Novel thermodynamically stable and oxidation resistant superhard coating materials, Surf. Coat. Technol. 86–87 (1996) 394–401.
[13] S.J. Bull, D.G. Bhat, M.H. Staia, Properties and performance of commercial TiCN coatings. Part 1: coating architecture and hardness modeling, Surf. Coat. Technol. 163–164 (2003) 499–506.
[14] Y.L. Su, S.H. Yao, Z.L. Leu, C.S. Wei, C.T. Wu, Comparison of tribological behavior of three films—TiN, TiCN and CrN—grown by physical vapor deposition, Wear 213 (1997) 165–174.
[15] H.O. Pierson, Titanium carbonitrides obtained by chemical vapor deposition, Thin Solid Films 40 (1977) 41–47.
[16] K. Matsuura, M. Kudoh, Surface modification of titanium by a diffusional carbo-nitriding method, Acta Mater. 50 (2002) 2693–2700.
[17] A.M. Peters, M. Nastasi, Effect of carrier gas on the deposition of titanium carbo-nitride coatings by a novel organo-metallic plasma immersion ion processing technique, Vacuum 67 (2002) 169–175.
[18] E. Damond, P. Jacquot, J. Pagny, $TiCxN_{1-x}$ coatings by using the arc evaporation technique, Mater. Sci. Eng. A 140 (1991) 838–841.
[19] D. Carole, N. Frety, S. Paris, D. Vrel, F. Bernard, R.-M. Marin-Ayral, Microstructural study of titanium carbonitride produced by combustion synthesis, Ceram. Int. 33 (2007) 1525–1534.
[20] M. Kamruddin, P.K. Ajikumar, S. Dash, A.K. Tyagi, B. Raj, Thermogravimetry-evolved gas analysis–mass spectrometry system for materials research, Bull. Mater. Sci. 26 (2003) 449–460.
[21] P.K. Ajikumar, M. Kamruddin, R. Nithya, P. Shankar, S. Dash, A.K. Tyagi, B. Raj, Surface nitridation of Ti and Cr in ammonia atmosphere, Scr. Mater. 51 (2004) 361–366.
[22] P.K. Ajikumar, A. Sankaran, M. Kamruddin, R. Nithya, P. Shankar, S. Dash, A.K. Tyagi, B. Raj, Morphology and growth aspects of Cr(N) phases on gas nitridation of electroplated chromium on AISI 316 LN stainless steel, Surf. Coat. Technol. 201 (2006) 102–107.
[23] K.N. Strafford, J.M. Towell, The interaction of titanium and titanium alloys with nitrogen at elevated temperatures. I. The kinetics and mechanism of the titanium-nitrogen reaction, Oxid. Met. 10 (1976) 41–67.
[24] U. Sen, Kinetics of titanium nitride coatings deposited by thermo-reactive deposition technique, Vacuum 75 (2004) 339–345.
[25] E. Metin, O.T. Inal, Kinetics of layer growth and multiphase diffusion in ion-nitrided titanium, Metall. Trans. A 20A (1989) 1819–1832.
[26] L. Vegard, Constitution of mixed crystals and the size of the atom, Z. Phys. 5 (1921) 17–26.
[27] H.O. Pierson, Handbook of Refractory Carbides and Nitrides, Noyes, Park Ridge, NJ, 1996.
[28] P.S. Weiser, S. Prawer, A. Hoffman, R.R. Manory, P.J.K. Paterson, S.-A. Stuart, Carbon diffusion in uncoated and titanium nitride coated iron substrates during microwave plasma assisted chemical vapor deposition of diamond, J. Appl. Phys. 72 (1992) 4643–4647.
[29] F. Anglezio-Abautret, B. Pellissier, M. Miloche, P. Eveno, Nitrogen self-diffusion in titanium nitride single crystals and polycrystals, J. Eur. Ceram. Soc. 8 (1991) 299–304.
[30] T.N. Blanton, C.L. Barnes, M. Lelental, The effect of X-ray penetration depth on structural characterization of multiphase Bi-Sr-Ca-Cu-0 thin films by X-ray diffraction techniques, Phys. C 173 (1991) 152–158.
[31] H.A. Wriedt, J.L. Murray, in: T.B. Massalski (Ed.), Binary Alloy Phase Diagrams, vol. 3, 1986, pp. 2705–2708.
[32] J.L. Murray, in: T.B. Massalski (Ed.), Binary Alloy Phase Diagrams, vol. 1, 1986, pp. 888–890.